

GSI or JRC – continuum or discontinuum modelling – some suggestions and some critique

Nick Barton

Nick Barton & Associates, Oslo, Norway

ABSTRACT: GSI has been applied for about 30 years and JRC for about 50 years. They are associated with either the Hoek-Brown based shear strength criterion for rock masses and *continuum modelling*, or with the Barton-Bandis based shear strength criterion for rock joints for use in *discontinuum modelling*. The latter, using input parameters JRC, JCS and ϕ_r provides for non-linear and block-size dependent shear-displacement and dilation-displacement behaviour, and non-linear closure-aperture behaviour, including the potential for coupled hydraulic flow modelling. The mismatch of hydraulic and physical apertures is emphasized, requiring lab-scale JRC_0 for the conversion. The paper provides some examples of joint-related behaviour in the case of tunnels, caverns and slopes. It also includes serious critique of GSI and the H-B based continuum modelling, due to the complex equations and the lack of representation of joint properties. So-called plastic zones are exaggerated around tunnels, and spoon-shaped slope failures belong in soil mechanics.

Keywords: modelling, rock masses, rock joints, JRC, GSI, shear strength.

1 INTRODUCTION

During past decades there have been periods with FEM dominated continuum modelling, followed by decades of DEM dominated discontinuum modelling when for instance UDEC, 3DEC and FRACMAN became available thanks to early developments by Cundall and Dershowitz. In more recent decades it seems that a return to continuum modelling of rock masses has been dominant and this has undoubtedly been in response to the commercial promotion of GSI and the Hoek-Brown equations for representing rock masses, and commercial software. In this paper some critical observations will be made to emphasize what is lost when attempting to select a representation of ‘geology’ in the GSI diagram. The actual ‘loss of geology’ is because there is a ‘homogenization’ of properties using Rocscience software to evaluate the ‘page-wide’ Hoek-Brown equations for ‘c’ and ‘ ϕ ’ and thence to FEM. It is doubted that such methods can help us understand fundamental rock behaviour, as so-called plastic zones around underground excavations are exaggerated, and spoon-shaped ‘failures’ of slopes in jointed rock are not observed unless the rock material is very weak.

Figure 1 illustrates the strong contrast between a continuum model and a discontinuum model when both are focused on the same problem: motorway and ramp tunnels in close proximity. The same rockmass deformation modulus are applied in each case, but the specified joints have normal and shear stiffnesses and can react to excavation under the applied stress.

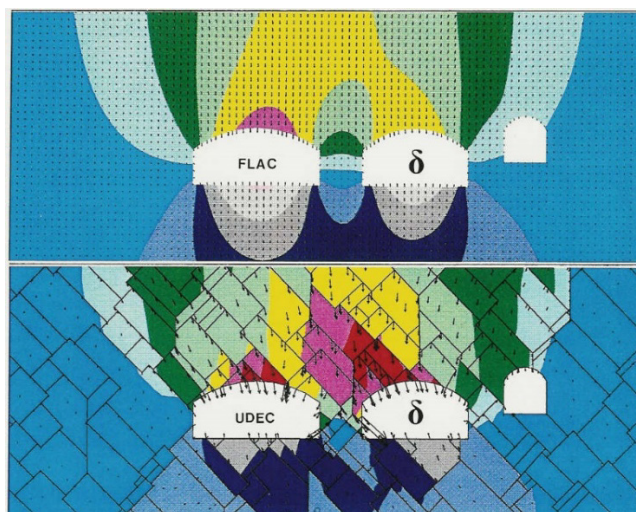


Figure 1. The contrasting information from a Cundall continuum model and from a Cundall discontinuum model, respectively FLAC-MC (2D) and UDEC-BB (2D). Anisotropy and local instability and eventual overbreak are clearly not a part of the continuum model. (Pers. comm. L. Backer, more than three decades ago). (MC refers to Mohr-Coulomb, and BB to Barton-Bandis representation of shear strength). $\delta_1/\delta_2 \approx 1/3$.

1.1 Elements of rock joint behaviour

When contemplating discontinuum modelling the deformability and shear behaviour of the component rock joints are clearly central themes of the discussion. Figure 2 illustrates in graphic format, how a rough tension fracture dilates and shears up to and beyond peak shear strength.

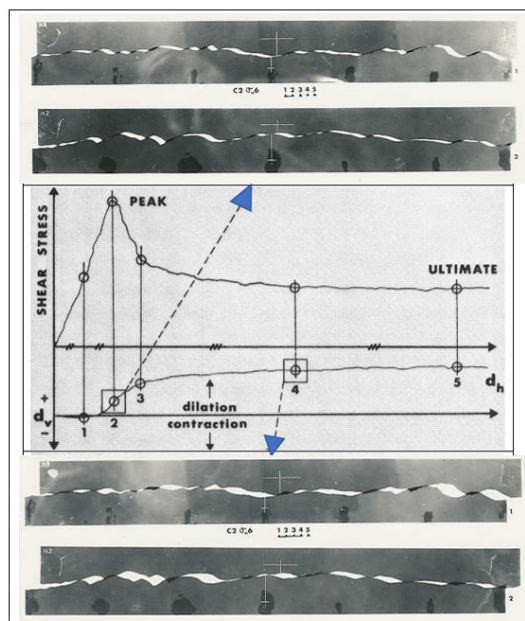


Figure 2. Model tension fractures (represented by their 2D photogrammetric profiles) with exaggerated roughness ($JRC = 20$, and an unweathered $JCS = 50\text{MPa}$) have been sheared under a scaled-up normal stress of 4.6MPa . Measured shear and dilation give approximate reconstruction of asperity crushing areas. The shear strength equation developed from such fractures was the forerunner of JRC and JCS. Barton, 1973.

1.2 Acquiring input data for joint modelling

An advantage of the ‘JRC-JCS’ model, referred to mostly as the Barton-Bandis criterion (Lei and Barton, 2021) is that input data has physical meaning, and is easily obtained. Figure 1 illustrates tilt tests (on joints and cores), Schmidt hammer tests (on clamped joints and cores), and profiling.

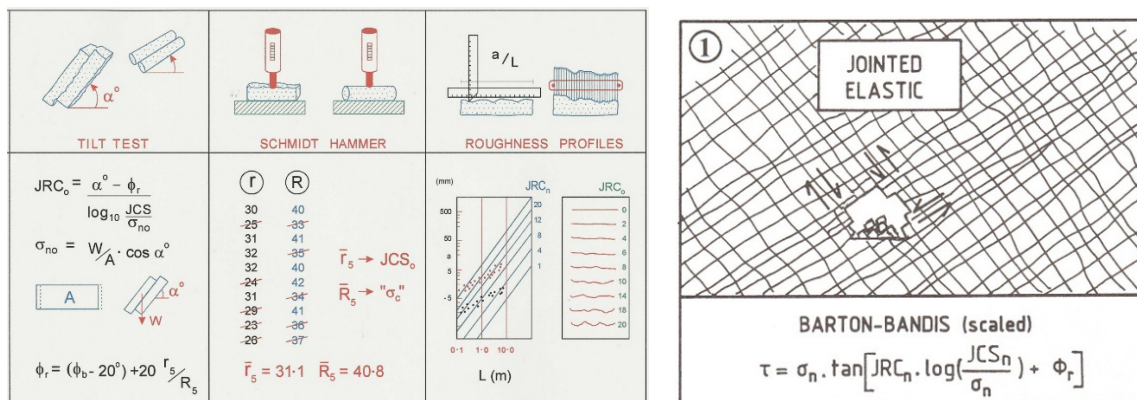


Figure 3. JRC, JCS and ϕ_r for input into the Barton-Bandis joint behaviour criterion can be obtained from simple index tests as illustrated: tilt tests (for JRC and ϕ_b), Schmidt hammer rebound (for JCS and, using r/R for ϕ_r), and finally roughness profiling for a visual small-scale record of each relevant joint set. For scaling JRC to the relevant block sizes, use the a/L amplitude/length method. JRC_n and JCS_n for natural block-size.

1.3 Joint deformation components and shear strength

Before any shear displacement the non-linear normal closure behaviour (the ‘N’ component) in Figure 4, determines the normal stiffness k_n . Ratios of normal and shear stiffness k_n/k_s may be in the range 10-50, but note the double scale-dependency of the shear stiffness k_s . The three rock mass representations with load-deformation sketches illustrate ‘a more challenging rock mechanics day’ than when using continuum modelling. They correspond to *in situ* loading test results which typically give concave or convex load vs. deformation behaviour, and linear behaviour for columnar basalt.

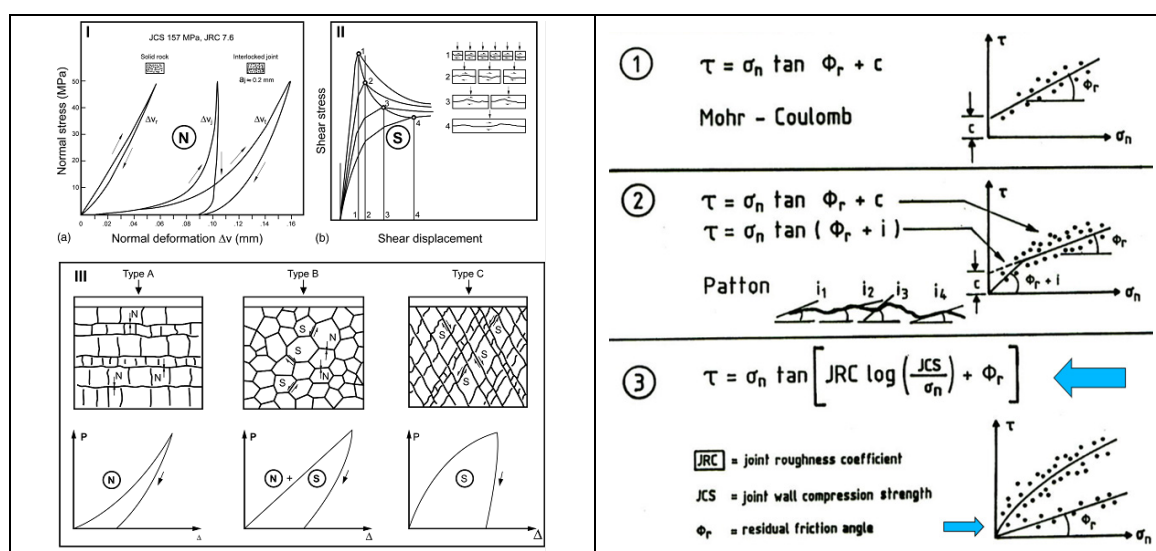


Figure 4. Left: The normal (N) and shear (S) components of joint behaviour (with allowance of scale effects). The three rock mass representations correspond to *in situ* loading test results. Bandis et al. 1983 and Barton, 1986. Right: Three peak shear strength criteria for rock joints include linear Mohr-Coulomb, bi-linear Patton (1966) and the non-linear JRC, JCS, ϕ_r criterion mostly introduced in Barton, 1973 but finalized with ϕ_r after direct shear tests with some partially weathered rock joints, following Barton and Choubey, 1977.

2 CHOOSING UDEC OR 3DEC OR FRACOD

Figure 5 shows an approximate method for judging the appropriate modelling method. Distinct element (jointed) models employing UDEC or 3DEC such as in Figures 6, 7 and 8 are expected to apply in a broad central area of jointed rock, representing a large majority of cases in many countries with competent igneous, metamorphic and sedimentary rock. Weak volcanic rocks largely devoid of jointing will obviously not be solved with such methods, and continuum modelling (e.g. FLAC and FEM) will apply. An excellent fracture mechanics BEM-based code: FRACOD belongs far right.

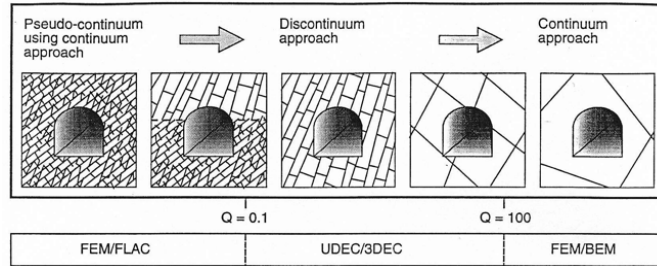


Figure 5. A approximate Q-value based scheme for choosing the appropriate type of model.

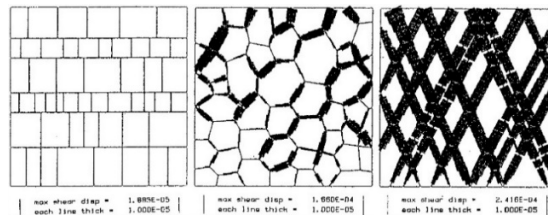


Figure 6. UDEC-BB models of the three idealized rock masses shown in Figure 4. The relative lack of shear (left), combined shear and closure (N+S) for the basalt columns, and greatly dominating shear (S) in the case of the conjugate jointing serve as illustration of serious differences between discontinuum and continuum.

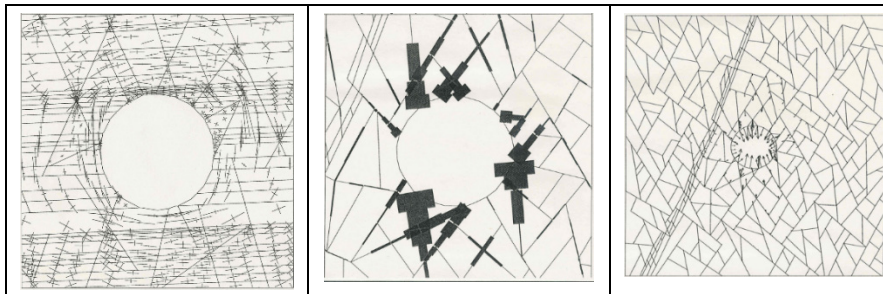


Figure 7. Representation of TBM drives in sandstone/siltstone (left) and welded tuff. The UDEC-BB models used input data based on the index tests shown in Figure 3, using numerous core samples of multiple joint sets.

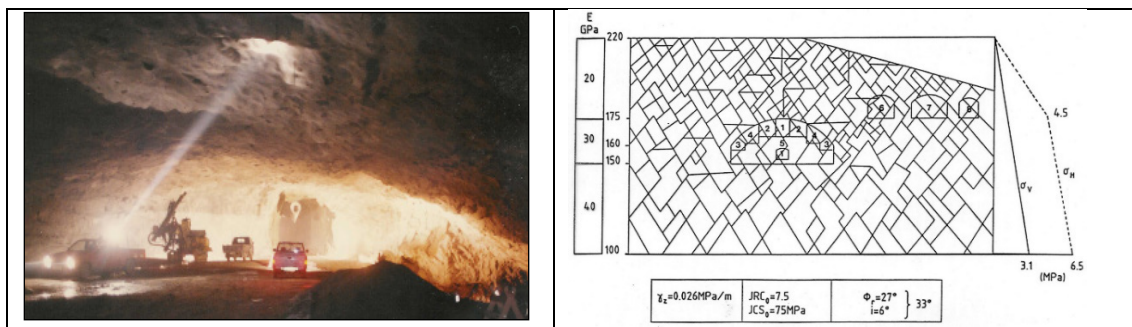


Figure 8. The challenging 62m span of the Gjøvik cavern, with UDEC-BB preparation using a digitized joint representation, depth dependent deformation moduli (ignored in the GSI world), and high horizontal stress.

3 CONTINUUM MODELLING PECULIARITIES

Many young people have apparently been persuaded by the ease of software and have assumed that ‘geology’ can be represented by Hoek’s well-known GSI, followed by application of the Hoek-Brown equations for shear strength. GSI is applied no less than 16-times in the equation for c' (yellow) and no less than 12-times in the equation for ϕ' (green). (See Figure 9). Extreme sensitivity to GSI is a negative aspect. The presence of a poorly defined ‘disturbance factor’ D (with values from 0 to 1) allows the user to obtain a wide range of results, especially in the case of the deformation modulus. (Equations not shown here and incorrectly taking no account for depth). Both V_p (P-wave velocity) and deformation modulus (E_{mass}) increase with depth, independent of the rock mass quality.

$c' = \frac{\sigma_{ci} [(1+2a)s + (1-a)m_b \sigma'_{3n}] (s + m_b \sigma'_{3n})^{a-1}}{(1+a)(2+a) \sqrt{1 + (6am_b (s + m_b \sigma'_{3n})^{a-1}) / (1+a)(2+a)}}$		
$\phi' = \sin^{-1} \left[\frac{6am_b (s + m_b \sigma'_{3n})^{a-1}}{2(1+a)(2+a) + 6am_b (s + m_b \sigma'_{3n})^{a-1}} \right]$		
$m_b = m_i \exp\left(\frac{GSI - 100}{28 - 14D}\right)$	$s = \exp\left(\frac{GSI - 100}{9 - 3D}\right)$	$a = \frac{1}{2} + \frac{1}{6} \left(e^{-\frac{GSI}{15}} - e^{-\frac{20}{3}} \right)$

Figure 9. The Hoek-Brown equations for representing the shear strength of rock masses when modelled as continua. These were derived from their empirical model of intact rock, not from rock joint behaviour. GSI actually appears sixteen times in the H-B equation for ‘ c' ’ and twelve times in the H-B equation for ‘ ϕ' ’!

The well-known GSI diagram of Hoek, showing some ‘rock mass sketches’ and a joint condition description (from Bieniawski) is not reproduced here due to the too small print. But suffice it to say that with a selected value of GSI typically between about 20 and 80, and values of the parameters m_b , s and a (see the subsidiary equations in Figure 9), and not forgetting a guessed value of D , a solution for the non-linear nature of the possible shear strength of the rock mass is obtained. Armed with the input data, a finite element program such as Phase 2, or the more recent RS2 from Rocscience is employed to calculate the isotropic continuum-based stress distribution and ‘plastic zone’ around an underground excavation, or the potential shear failure beneath a rock slope.

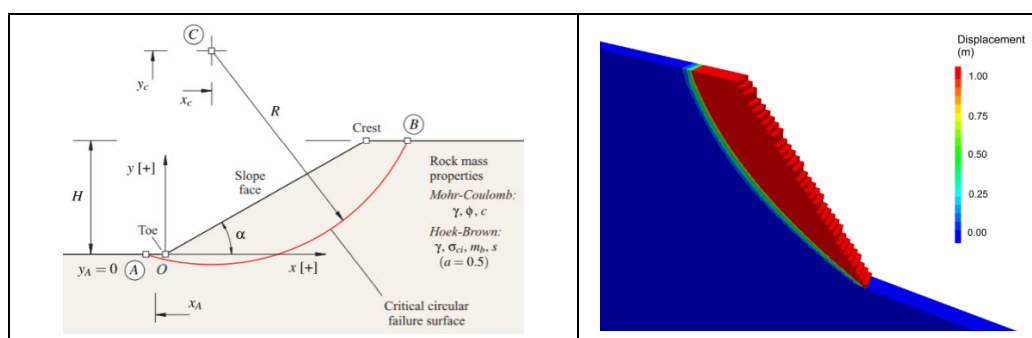


Figure 10. Spoon-shaped slope failure surfaces from analytical (left, Carranza-Torres, 2021) and numerical modelling (a FLAC-3D slice from Styles et al. 2022) have something in common in that both use H-B (from GSI quantification) to evaluate M-C parameters. The numerical model is more sophisticated with consideration of strain-dependent modulus and strain-dependent dilation, using ‘the best aspects of H-B and M-C’.

However, slopes in jointed rock do not fail like continua, so one will only see ‘spoon-shaped’ failure in soils or in rockfill, or in the case of extremely weak materials like saprolite or lake-bed sediments. They cannot fail like this if competent jointed (and maybe faulted) rock is present. Usually, as in the case of the huge slide illustrated in Figure 11, there will be major structure involved too. In this case a major (continuous) fault zone provided a 1/2 km long plane of sliding. The huge Bingham slide involved 70,000,000 m³ of waste rock and ore which failed in two events and involved progressive

failure. There were no casualties, and most equipment was saved. It has been misinterpreted as a ‘circular’ failure by some authors, as have some other large failures. More care is suggested.



Figure 11. The massive Bingham Canyon mine open pit failure involved an adverse and unloaded ‘nose’ in its upper 1/3rd and a major ½ km long fault surface in the upper region of the extraordinary 3km long failure path. Such failures can be understood by using up to four of the components of shear strength shown in Figure 12.

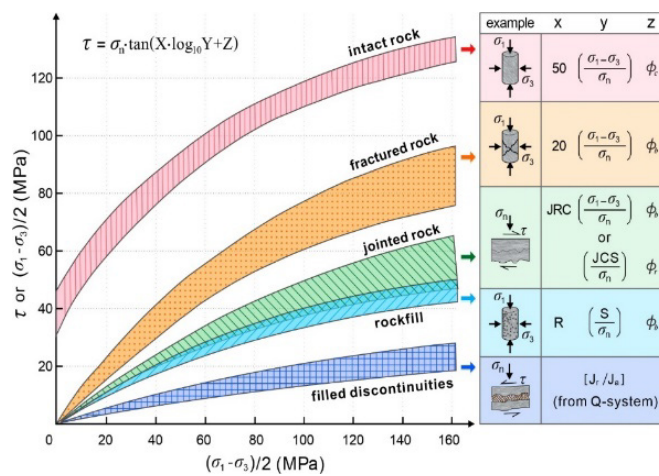


Figure 12. Shear strength components of a jointed rock mass. The CcSs criterion, involving breakage of cohesion (‘crack’), shearing on these fresh surfaces (‘crunch’), sliding on kinematically capable rock joints (‘scrape’) and finally sliding on adversely oriented filled discontinuities or faults (‘swoosh’). Barton, 2022.

REFERENCES

- Bandis, S., Lumsden, A.C. & Barton, N. 1983. Fundamentals of rock joint deformation. *Int. J. Rock Mech. Min. Sci. and Geomech. Abstr.* Vol. 20: 6: 249-268.
- Barton, N. 1973. Review of a new shear strength criterion for rock joints, *Engineering Geology*, Elsevier, Amsterdam, Vol. 7, pp. 287-332. Also NGI Publ. 105, 1974.
- Barton, N. & Choubey, V. 1977. The shear strength of rock joints in theory and practice. *Rock Mechanics* 1/2:1-54. Vienna: Springer.
- Barton, N. 1986. Deformation phenomena in jointed rock. 8th Laurits Bjerrum Memorial Lecture, Oslo. *Geotechnique*, Vol. 36: 2: 147-167.
- Barton, N. 2022. Keynote Lecture: Continuum or Discontinuum – That is the Question. 26p. *IX Latin American Rock Mechanics Symposium, Asuncion*, Paraguay.
- Carranza-Torres, C. 2021. Computational tools for the analysis of circular failure of rock slopes. Keynote Lecture. In Proceedings of EUROCK 2021, Torino, Italy.
- Lei, Q. and N. Barton, 2022. On the selection of joint constitutive models for geomechanics simulation of fractured rocks. *Computers and Geotechnics*, Volume 145, May 2022, 10p.
- Patton, F.D. 1966. Multiple modes of shear failure in rock. *Proc. 1st ISRM Congress*, Lisbon; Vol.1, 509-513.
- Styles, T. D., Jackson, S.J. & Vakili, E. 2022. A tool to estimate factor of safety for varying slope height and angle in specific rock mass conditions. *Slope Stability 2022 Conference*, Tucson, USA. 13p.